JOURNAL OF MATERIALS SCIENCE 33 (1998) 4455–4459

Sol-gel processed barium titanate ceramics and thin films

H. B. SHARMA*, A. MANSINGH
Department of Physics and Astrophysics, University of Delhi, Delhi 110 007, India
E-mail: libmu@cal.vnsl.net.in

Ferroelectric barium titanate ($BaTiO_3$) ceramics and thin films have been prepared from barium acetate ($Ba(CH_3COO)_2$) and titanium (IV) isopropoxied ($Ti((CH_3)_2CHO)_4$) precursors by a sol–gel technique. The as-grown powder and thin films were found to be amorphous, which crystallized to the tetragonal phase after annealing at 700 °C in air for 1 h. Both the ceramics and thin films showed well-saturated polarization–field (*P–E*) hysteresis loops at room temperature. The value of the spontaneous polarization, P_S, remnant polarization, P_r, and coercive field, E_c, of the ceramics and thin films determined from the *P–E* hysteresis loop were found to be 19.0 and 12.6; 14.0 and 3.2 $\mu G\,cm^{-2}$, and 30 and 53 $kV\,cm^{-1}$, respectively. The coercive field of the film determined from the capacitance–voltage, *C–V*, characteristics is slightly lower than that determined from the *P–E* hysteresis loop (43 $kV\,cm^{-1}$). The room-temperature dielectric constant, ε, of the ceramics and films was found to be 1135 and 370, respectively. Both the films and ceramics showed dielectric anomaly peaks at 125 °C, showing ferroelectric to paraelectric phase transition. © *1998 Kluwer Academic Publishers*

1. Introduction

Ferroelectric bulk ceramics and single crystals have found wide applications in many electronic, acousto-optic, piezoelectric devices [1, 2]. Recently there has been considerable interest in the ferroelectric thin films due to possible applications in integrated devices [3–6]. The advantages of thin-film devices include low operating voltages, high switching speeds and possible integration with the existing semiconductor technology. With the advancement of thin-film technology, attempts have been made to prepare near-bulk-quality ferroelectric thin films for device applications. However, the properties of the films showed a sharp decrease as compared to their ceramic counterparts. The properties of ferroelectric bulk ceramics and thin films have been widely investigated [1, 7]. However, there is virtually no report of the studies on the basic properties of the bulk ceramics and thin films prepared by the same technique. In this paper, we report the ferroelectric and dielectric properties of sol–gel processed $BaTiO_3$ ceramics and thin films.

The most common method for making $BaTio_3$ ceramics is the conventional solid-state reaction method [7]. Recently, the sol–gel technique has been utilized for the fabrication of ferroelectric $BaTiO_3$ bulk powder and ceramics [8, 9]. The advantages of the sol–gel technique include fine particle size, easy compositional control and low processing temperature. Various deposition techniques, such as sputtering [10], evaporation [11], metalo-organic chemical vapour deposition (MOCVD) [12], sol–gel [13], etc, have been utilized for the fabrication of ferroelectric $BaTiO_3$ thin films. Among the various techniques, sol–gel is gaining interest for the fabrication of ferroelectric films due to low equipment cost and ease of integration with the already existing semiconductor technology.

2. Experimental procedure

The source chemicals containing the metal components (barium and titanium) were barium acetate [$Ba(CH_3COO)_2$] and titanium (IV) isopropoxide [$Ti((CH_3)_2CHO)_4$]. Barium acetate was first dissolved in acetic acid [CH_3COOH] and then diluted with 2-methoxyethanol [$CH_3OCH_2CH_2OH$]. An equimolar amount of $Ti((CH_3)_2CHO)_4$ was then added to the above solution, keeping it constantly stirred and filtered using microfibre glass filter paper. The filtrate was used as the stock solution for the preparation of the $BaTiO_3$ ceramics and thin films. For the preparation of the ceramics, the stock solution was set aside (for about 24 h) until a white opaque gel was obtained. The gel was converted to white powder after drying at 350 °C. The resulting powder was then annealed at 700 °C in air for 1 h for crystallization. The ceramic samples were prepared by pressing the powder, using a pressure of 1.25×10^3 $kg\text{-}cm^{-2}$, in the form of circular discs (1 cm diameter and 0.1 cm thick) and sintering at 1300 °C for 2 h. Thin films were

* *Present address*: Department of Physics, Manipur University, Canchipur, Imphal 795 003, India; also Department of Physics, G.P. Women's College, Imphal 795 001, India.

prepared on $Pt/Ti/SiO_2/Si$ (PS) substrates by spin casting of the stock solution at 4000 r.p.m. for 30 s. Following the deposition, the films were heat treated for 5 min at 350 °C in air ambient. Thicker films were prepared by repeating the deposition cycle (the thickness of each coating being 0.125 μm). The films were then annealed at different temperatures for 1 h by using a conventional furnace.

The structure of the ceramics and thin films were characterized by X-ray diffraction technique using a Phillips (model PW 1840) X-ray diffractometer. The microstructure of the samples was investigated by using a Jeol (model JSM 840) scanning electron microscope. The dielectric properties were measured by using a GR 1615 Capacitance Bridge. The polarization–field hysteresis was measured at 50 Hz using a Sawyer–Tower circuit. The capacitance–voltage and conductance–voltage characteristics were measured using a Parc CV plotter (model 410). All the electrical measurements were carried out in the metal–ferroelectric–metal (MFM) configuration. Ceramic samples were prepared by electroding the sintered discs with silver paint and poling in oil at 150 °C for 2 h using a poling field of 30 kV cm^{-1}. Thin-film samples having a thickness of 0.375 μm deposited on PS substrates. Gold circular electrodes of area 1.96×10^{-3} cm^2 were deposited by vacuum evaporation on the top of the films.

3. Results and discussion

3.1. Structure and microstructure

The as-fired powder was found to be amorphous and had a particle size < 1 μm. Annealing at 700 °C for 1 h gave polycrystalline $BaTiO_3$ powder, as shown in the X-ray diffraction (XRD) pattern of Fig. 1. The XRD peak positions are in good agreement with that of tetragonal $BaTiO_3$ powder [14]. Upon pressing and sintering, the particles coalesce to form large well-defined crystallites (Fig. 2a). Similar to the powder, the as-fired film was also found to be amorphous. The films were crystallized to tetragonal phase after annealing at 700 °C for 1 h in air.

3.2. Ferroelectric properties

3.2.1. Polarization–field (P–E) hystereis

The room-temperature polarization–field hysteresis of the ceramics showed well-saturated loops (Fig. 3a). The values of the remnant polarization, spontaneous polarization and coercive field determined from Fig. 3a are reported in Table I. It may be noted that the polarization values of the ceramics are lower than that of the single crystal, whereas the coercive field is higher. This may be attributed to the existence of the non-ferroelectric layers at the metal–ferroelectric interfaces and grain boundaries [15]. However, the polarization values of the ceramics are comparable to the best-reported values of $BaTiO_3$ ceramics prepared by the solid-state reaction method [7]. The thin film also showed a well-saturated P–E hysteresis loop at room temperature (Fig. 3b). The loop is slim as compared to that of the ceramic. The values of P_r, P_s and E_c are reported in Table I. It may be pointed out that the spontaneous polarization and remnant polarization of the films are much lower than that of ceramics, whereas the coercive field is higher. The lower value of the polarization in the films may be due to the smaller

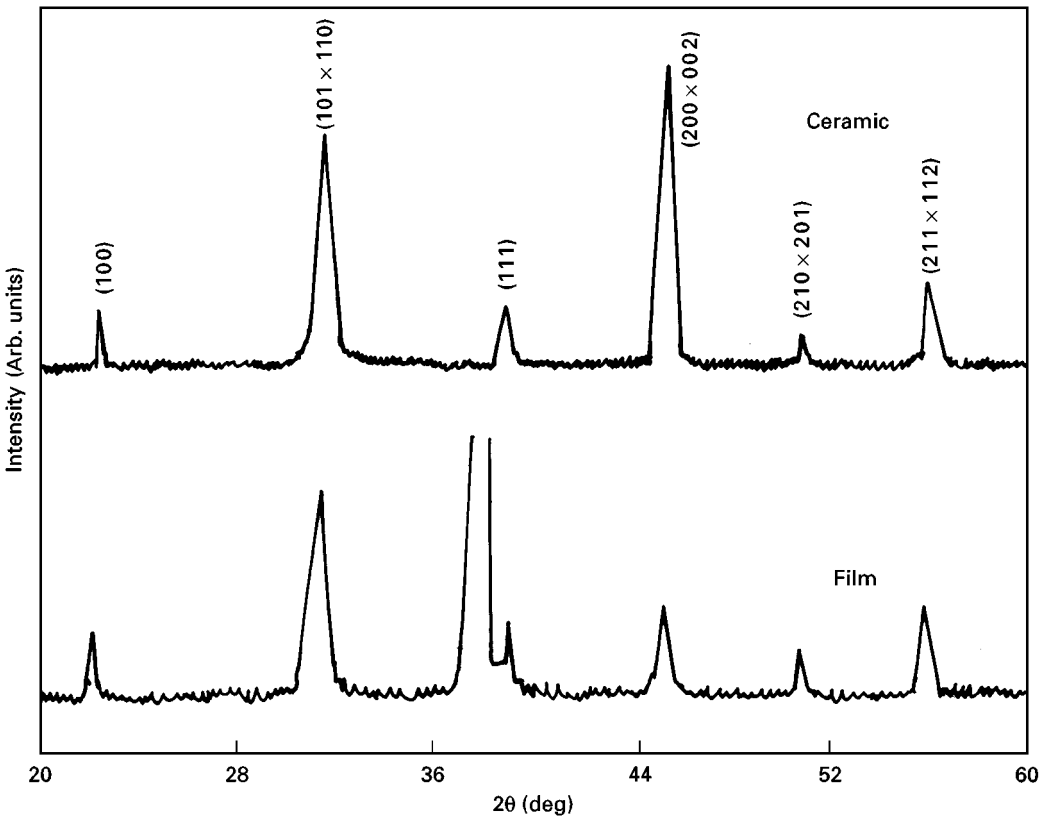

Figure 1 X-ray diffraction pattern of sol–gel processed $BaTiO_3$ ceramic (sintered at 1300 °C for 2 h) and thin film deposited on platinized silicon substrate.

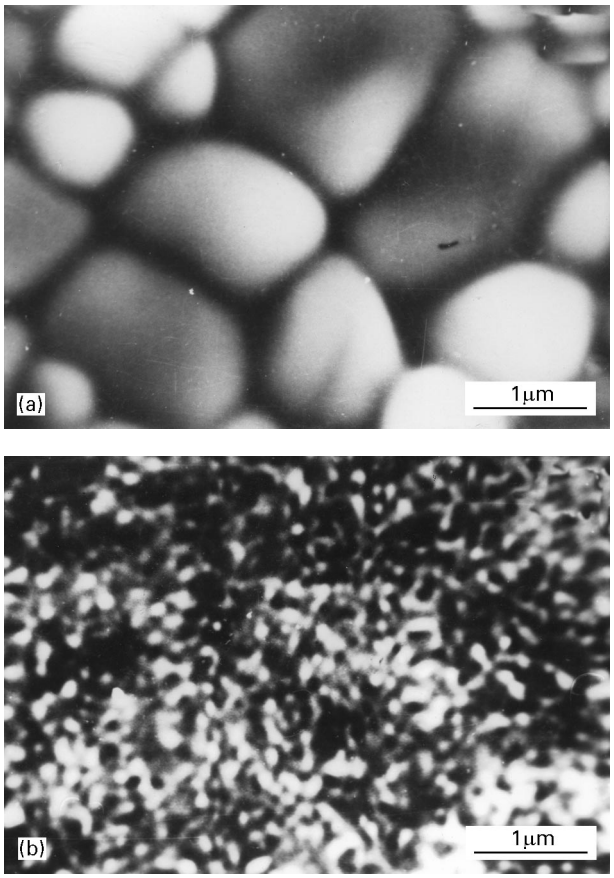

Figure 2 Scanning electron micrographs of $BaTiO_3$ (a) ceramic and (b) thin film deposited on a PS substrate.

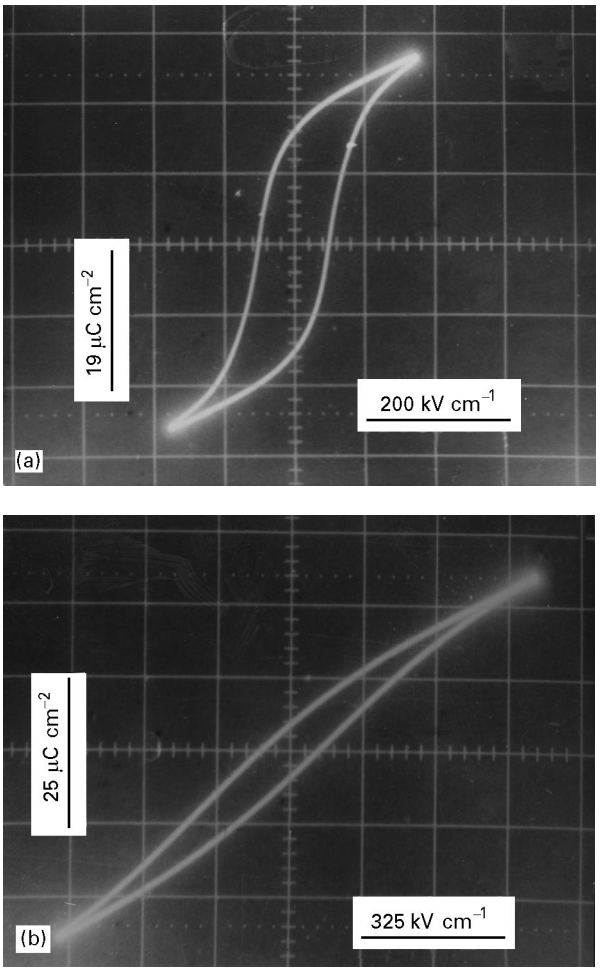

Figure 3 Polarization–field hysteresis loops of $BaTiO_3$ (a) ceramic and (b) thin film.

grain size and lower packing density of the films as compared to that of the ceramics. Higher values of the coercive field in ferroelectric films than their ceramic counterparts have been reported in the literature by several workers [16, 17]. A decrease in the polarization and increase in E_c with decreasing thickness has also been reported in TGS single crystal [15]. This has been attributed to the existence of non-ferroelectric surface layer at the crystal–electrode interface. The existence of non-ferroelectric layers at the metal–film interface and at the grain boundaries may be responsible for the higher value of the coercive field and lower value of the polarization in the films.

3.2.2. Capacitance–voltage characteristics

The investigation of *d.c.* electric field dependence of the dielectric constant, ε, and loss tangent, tanδ, is one of the methods for gaining insight into the behaviour of the ferroelectric materials and has been used to characterize ferroelectric thin films [18, 19]. The *d.c.* field dependence of ε and tanδ of the films were investigated by measuring capacitance–voltage, *C–V*, and conductance–voltage, *G–V*, characteristics. The *C–V* and *G–V* characteristics of the ceramic samples were not measured, due to the requirement of high *d.c.* biasing field. Fig. 4 shows the room-temperature *C–V* and *G–V* characteristics of $BaTiO_3$ film fabricated on a PS substrate. Similar to the *P–E* hysteresis loop (Fig. 3b), the *C–V* plot also showed a hysteresis effect. In either of the two (i.e. left and right) branches, both *C* and *G* display bell-like curves and have much reduced values at high biasing fields of positive and negative polarity. They also exhibit a maximum at a *d.c.* bias, which can be regarded as the coercive field in the corresponding *P–E* hysteresis loop. The calculated value of coercive field, E_{cl}, was found to be 45 kV cm^{-1}, which is slightly lower than that determined from *P–E* hysteresis measurements. This may be attributed to the frequency and field dependency of the ferroelectric properties of the film. The existence of the *C–V* and *G–V* hysteresis confirmed the ferroelectricity in our films.

3.3. Dielectric properties

The room-temperature dielectric constant, ε, and loss tangent, tanδ, of the ceramics at 1 kHz were found to be about 1135 and 0.012, respectively. There is small frequency dispersion on the dielectric constant, as shown in Fig. 5. Similar behaviour has been observed in the majority of ferroelectric ceramics [7]. The value of ε of the ceramics is lower than that reported for $BaTiO_3$ single crystal [7]. The difference in the dielectric constants of the ceramics and $BaTiO_3$ single crystal may be attributed to the structural and compositional variances. In addition to those mentioned above, porosity and the existence of low dielectric constant non-ferroelectric layers at the

TABLE I Ferroelectric properties of $BaTiO_3$ ceramic and thin films

Sample	Remnent polarization, P_r(μC cm^{-2})	Spontaneous polarization, P_s(μC cm^{-2})	Coercive field (P–E), E_c(kV cm^{-1})	Coercive field (C–V), E_{c1}(kV cm^{-1})	Reference
Single crystal	20.0	25.0	10	–	[8]
Sol–gel ceramic	12.6	19.0	30	–	Present work
Sol–gel film	3.2	14.0	53	45	Present work

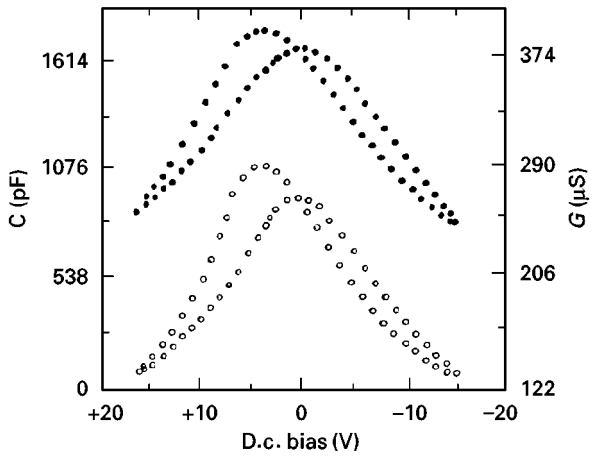

Figure 4 (●) Capacitance–voltage (C–V) and (○) conductance–voltage (G–V) characteristics of $BaTiO_3$ thin film at room temperature.

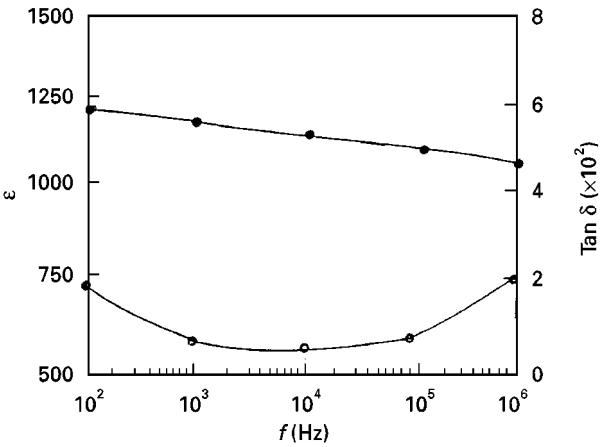

Figure 5 Variation of (●) dielectric constant, ε, and (○) loss tangent, tan δ, of $BaTiO_3$ ceramic with frequency.

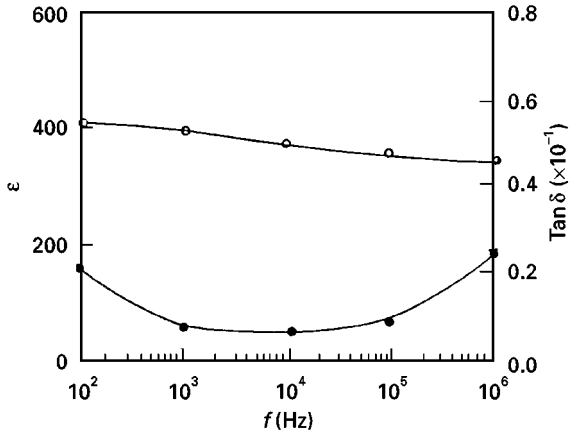

Figure 6 Variation of (○) dielectric constant, ε, and (●) loss tangent, tan δ, of $BaTiO_3$ film with frequency.

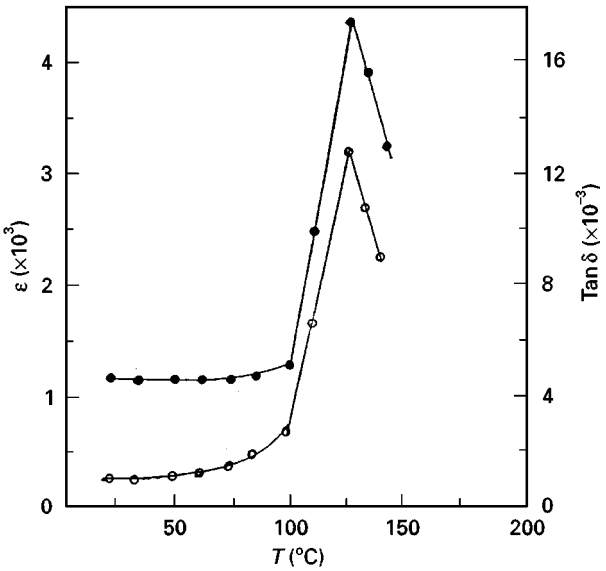

Figure 7 Variation of (●) dielectric constant, ε, and (○) loss tangent, tan δ, of $BaTiO_3$ ceramic with temperature.

metal–ferroelectric interface and grain boundaries [15], may also play an important role in reducing the dielectric constant of the ceramics. The lower values of ε in ferroelectric ceramics as compared to their single-crystal counterparts have been widely documented in the literature [1, 7]. The room-temperature dielectric constant and loss tangent of the film at 1 kHz was found to be 370 and 0.015. Similar to the ceramics, ε of the films also shows a weak frequency dispersion (Fig. 6). It may be noted that the value of ε of the film is much lower than that of the ceramics, whereas the value of tan δ is higher. Earlier workers [20–25] have reported similar results. The same argument that was mentioned in the case of ceramics may be applied in explaining the lowering of ε in the films. However, further lowering in the dielectric constant of the films suggests that the influence of the non-ferroelectric layers at the grain boundaries and metal–ferroelectric interfaces makes a greater contribution in determining the dielectric constant of the material.

The effects of temperature on the dielectric constant of the ceramics and films were also investigated. Figs 7 and 8, respectively, show the variation ε and tan δ of the ceramics and thin film with temperature at 1 kHz. It may be pointed out from Fig. 7 that both ε and tan δ of the ceramics showed a peak at 125 °C, showing a phase transition from ferroelectric to paraelectric.

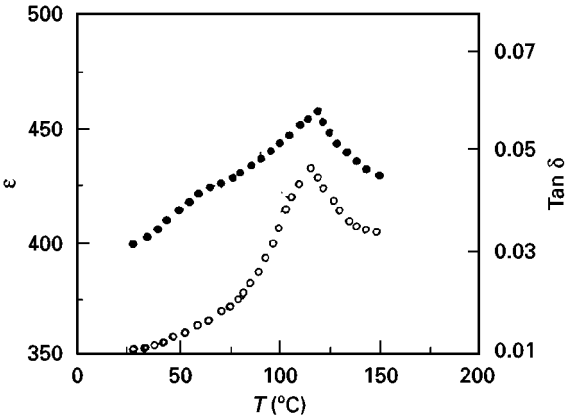

Figure 8 Variation of (●) dielectric constant, ε, and (○) loss tangent, tan δ, of $BaTiO_3$ thin film with temperature.

The peak is broad and low in magnitude as compared to that of $BaTiO_3$ single crystal [7]. The peak is more diffuse and lower in magnitude in the case of the films. Similar results have been observed in the majority of ferroelectric films [24, 25]. The lowering and broadening of the dielectric anomaly peak in the ceramics and thin film may be attributed to lower density, structural and chemical disorder or the existence of space-charge layers at the film–electrode interface and grain boundaries. However, the above argument is purely speculative, and more studies on the ceramics and thin films having different structures, compositions, grain sizes, etc., are needed to obtain a conclusive picture.

4. Conclusion

Ferroelectric $BaTiO_3$ ceramics and thin films have been prepared by the sol–gel technique. The as-grown powder and thin films were found to be amorphous, which crystallized to tetragonal phase after annealing at 700 °C for 1h. Both the ceramics and thin films showed well-saturated *P–E* hysteresis loops at room temperature. The values of room-temperature spontaneous polarization, remnant polarization and coercive field of the ceramics and thin films determined from the *P–E* hysteresis loop, were found to be 19.0 and 12.6, 14.0 and 3.2 μC cm^{-2}, and 30 and 53 kV cm^{-1}, respectively. The coercive field of the film determined from the *C–V* characteristics is slightly lower than that determined from the *P–E* hysteresis loop. The room-temperature dielectric constant of the ceramics and films were found to be 1135 and 370, respectively. Both the films and ceramics showed dielectric anomaly peaks at 125 °C showing ferroelectric to paraelectric phase transition.

Acknowledgement

The financial help to H. B. K. S. by the University Grants Commission (INDIA) is greatly acknowledged.

References

1. J. C. BURFOOT and G. W. TAYLOR, in "Polar Dielectrics and their Applications" (Macmillan, London, 1979) p. 76
2. M. E. LINES and M. GLASS, in "Principles and Applications of Ferroelectric and Related Materials" (Clarendon Press, Oxford, 1977) Ch. 4.
3. S. B. KRUPANIDHI, H. HU and C. V. R. V. KUMAR, *J. Appl. Phys.* **71** (1992) 376.
4. L. H. PARKER and A. F. TASCH, *IEEE Circ. Dev. Mag.* **1** (1990) 17.
5. A. MANSINGH, *Ferroelectrics* **102** (1990) 69.
6. P. K. LARSEN, D. J. DORMNS, G. W. TAYLOR and P. J. VEDHOVEN, *J. Appl. Phys.* **76** (1994) 2405.
7. B. JAFEE, W. R. COOK and H. JAFEE, in "Piezoelectric Ceramics" (Academic Press, London, 1971) p. 74.
8. P. PHULE and R. H. RISBUD, *Mater. Res. Soc. Symp. Proc.* **121** (1991) 275.
9. *Idem.*, *Adv. ceram. Mater.* **3** (1988) 123.
10. J. K. PARK and G. GRANNMEN, *Ferroelectric* **10** (1976) 315.
11. B. S. KWAK, K. ZHANG, R. P. BOYD, A. ERBIL and B. J. WILKENS, *J. Appl. Phys.* **69** (1991) 767.
12. M. N. KAMALSANAN, S. CHANDRA, P. C. JOSHI and A. MANSINGH, *Appl. Phys. Lett.* **60** (1991) 1022.
13. A. MANSINGH and G. RAI, *Can. J. Phys.* **54** (1976) 2050.
14. ASTM 5-0621 (American Society for Testing and Materials, Philadelphia, PA). (Edited by Joint Committee on Powder Diffraction Standards, Swarthm ore, USA 1991).
15. A. MANSINGH and G. RAI, *Can. J. Phys.* **54** (1976) 2050.
16. A. MANSINGH, *Bul. Mater. Sci.* **2** (1990) 325.
17. F. JONA and G. SRINE, in "Ferroelectric Crystals" (Dover, New York, 1993) p. 278.
18. H. HU and S. B. KRUPANIDHI, *J. Appl. Phys.* **74** (1993) 3373.
19. K. SREENIVAS and A. MANSINGH, *ibid.* **62** (1987) 4475.
20. H. F. CHENG, M. H. YEH, K. S. LIU and I. N. LIN, *Jpn. J. Appl. Phys.* **32** (1993) 5656.
21. A. S. SHAIKH, R. W. VEST and G. M. VEST, *IEEE Trans. Ultra. Freq. Control* **36** (1989) 407.
22. V. S. DHARMADHIKARI and W. W. GRANNEMANN, *J. Appl. Phys.* **53** (1982) 8988.
23. P. LI and T.-M. LU, *Appl. Phys. Lett.* **24** (1985) 401.
24. Y. IJJIMA, *Jpn J. Appl. Phys.* **24** (1985) 401.
25. T. KAWANO, T. SEI and T. TSUCHIA, *ibid.* **31** (1991) 2178.

Received 23rd August 1996
and accepted 22 April 1998